SOFT QCD RESULTS FROM THE CMS EXPERIMENT*

Paolo Bartalini

on behalf of the CMS Collaboration

NTU — National Taiwan University
Roosevelt Road, 10617 Taipei, Taiwan (ROC)

(Received November 24, 2011)

The CMS soft QCD results in proton–proton collisions at different LHC centre-of-mass energies are reviewed. The first part of the review focuses on the basic kinematic measurements of charged tracks and identified hadrons in minimum bias proton–proton interactions. The second part reports the short- and long-range correlation studies with emphasis on the results exploiting a special trigger specifically developed for large multiplicity events. The third part concentrates on the underlying event phenomenology in jet and Drell–Yan events. Some relevant highlights from the CMS heavy ion program are also discussed.

DOI:10.5506/APhysPolB.42.2657
PACS numbers: 13.85.–t, 13.85.Hd, 13.85.Ni, 25.75.Nq

1. Measurements of particle yields and kinematic distributions

Measurements of particle yields and kinematic distributions are an essential first step in exploring a new energy regime of particle collisions. Such studies contribute to our understanding of the physics of hadron production, including the relative roles of soft and hard scattering contributions, and help construct a solid foundation for other investigations. In the complicated environment of LHC proton–proton collisions, firm knowledge of the rates and distributions of inclusive particle production is needed to distinguish rare signal events from the much larger backgrounds of soft hadronic interactions. They also serve as points of reference for the measurement of nuclear-medium effects in PbPb collisions in the LHC heavy ion program.

These early low p_{T} QCD measurements mostly rely on the performances of the tracking and triggering systems. A detailed description of the CMS detector is available in Ref. [1].

* Presented at the LI Cracow School of Theoretical Physics "Soft Side of the LHC", Zakopane, Poland, June 11–19, 2011.

Most of the results presented in this section refer to inelastic non-single-diffractive (NSD) interactions and are based on an event selection that retains a large fraction of the non-diffractive (ND) and double-diffractive (DD) events, while disfavouring single-diffractive (SD) events.

The methodologies which push the cluster counting below 50 MeV/c and allow for track reconstruction (with p_{T} measurement) from 75 MeV/c have been introduced in the first CMS paper on collision data, reporting the transverse momentum and pseudorapidity distributions of charged hadrons in proton–proton interactions at $\sqrt{s} = 0.9$ and 2.36 TeV [2], subsequently complemented by the extension of the same measurement at 7 TeV [3]. Calorimeter-based high-transverse-energy triggers are employed to enhance the statistical reach of the high-p_{T} measurements [4].

The CMS charged multiplicity studies [5] rely on a Bayesian unfolding technique taking into account the detector effects [6]. Traditionally, the s dependence of the multiplicity distributions P_n and its moments has been much discussed [7] in relation to Koba–Nielsen–Olesen (KNO) scaling [8,9]. In this framework, one studies the KNO function $\Psi(z) = \langle n \rangle P_n$, where $z = n/\langle n \rangle$. The multiplicity distributions are shown in KNO form in Fig. 1 for a large pseudorapidity interval of $|\eta| < 2.4$, where we observe a strong violation of KNO scaling between $\sqrt{s} = 0.9$ TeV and 7 TeV, and for a small pseudorapidity interval of $|\eta| < 0.5$, where KNO scaling holds. These CMS observations and the older phenomenology from SPS and LEP point to the increasing importance of multiple parton interactions (MPI) in high energy hadron–hadron inelastic collisions at high $\sqrt{s}$.

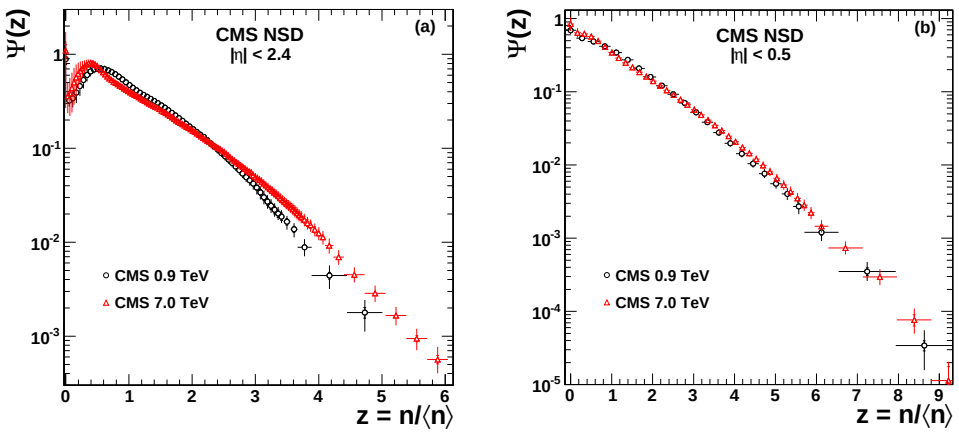

Fig. 1. The charged hadron multiplicity distributions in KNO form at $\sqrt{s} = 0.9$ and 7 TeV in two pseudorapidity intervals, (left) $|\eta| < 2.4$ and (right) $|\eta| < 0.5$.

The measurement of particle yields and spectra is extended to strange mesons and baryons (K^0_S, Λ, Ξ^-) at centre-of-mass energies of 0.9 and 7 TeV [10]. By fully exploiting the low-momentum track reconstruction capabilities of CMS, the transverse momentum distribution of these strange particles is reconstructed down to zero. As the strange quark is heavier than up and down quarks, production of strange hadrons is generally suppressed relative to hadrons containing only up and down quarks. The amount of strangeness suppression is an important component in Monte Carlo models. Pre-LHC tunes are generally found to underestimate strangeness production. If a quark-gluon plasma or other collective effects were present, we might expect an enhancement of double-strange baryons to single-strange baryons and/or an enhancement of strange baryons to strange mesons. However, as shown in Fig. 2, the production ratios $N(\Lambda)/N(K^0_S)$ and $N(\Xi^-)/N(\Lambda)$ *versus* transverse momentum show no change with centre-of-mass energy. The same conclusion is drawn when looking at the ratios against the pseudorapidity.

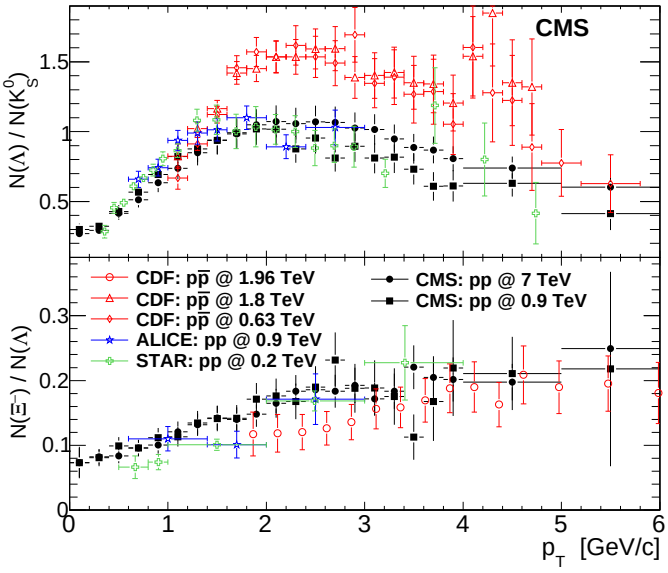

Fig. 2. Ratio of Λ to K^0_S production (top) and Ξ^- to Λ production (bottom) *versus* p_T. The CMS, ALICE [11], and STAR [12] error bars include the statistical and systematic uncertainties. The CDF error bars include the statistical uncertainties for $N(\Lambda)/N(K^0_S)$ [13] and the statistical and systematic uncertainties for $N(\Xi^-)/N(\Lambda)$ [14]. The CDF $N(\Lambda)/N(K^0_S)$ bin sizes are doubled to reduced fluctuations. For experiments in which the binning for Λ and Ξ^- is different (ALICE and STAR), bins are merged to provide common bin ranges in the $N(\Xi^-)/N(\Lambda)$ distribution.

The multiplicity density per unit of pseudorapidity $dN_{\mathrm{ch}}/d\eta$ is also measured using the 2.76 TeV-per-nucleon PbPb collision data recorded by the CMS detector in runs without magnetic field [15].

In studies with heavy ions, it is important to determine the degree of overlap of the two colliding nuclei, the so-called centrality of the interaction. Centrality is estimated using the sum of transverse energy in towers from both Hadron Forward (HF) calorimeters at positive and negative z positions. The distribution of the total transverse energy was used to divide the event sample into bins, each representing 5% of the total nucleus–nucleus interaction cross-section. The bin corresponding to the most central events (*i.e.* smallest impact parameter) is the 0–5% bin, the next one is 5–10% and so on. The distribution of the HF signal, along with the cuts used to define the various event classes, is shown in the left panel of Fig. 3. The centrality binning can be correlated with more detailed properties of the collision. The quantity of interest for this measurement is the total number of nucleons in the two Pb nuclei that experienced at least one inelastic collision, N_{part}, which is obtained using a Glauber Monte Carlo simulation [16, 17] with the same parameters as in Ref. [18].

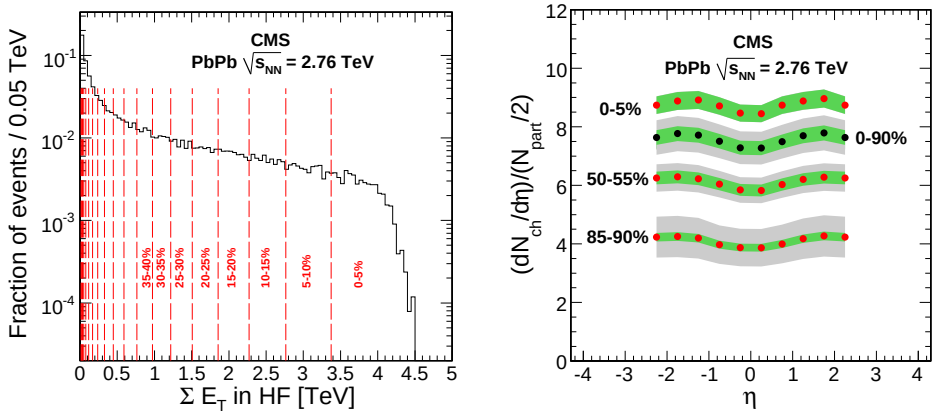

Fig. 3. Left: Distribution of the total transverse energy in the Hadron Forward calorimeters used to determine the centrality of the PbPb interactions. The centrality boundaries for each 5% centrality interval are shown by the dashed lines. Right: Measured $dN_{\mathrm{ch}}/d\eta/(N_{\mathrm{part}}/2)$ distributions from this analysis as a function of η in various centrality bins.

The measured charged multiplicity distribution per unit of pseudorapidity and participating nucleon pairs as a function of η, $(dN_{\mathrm{ch}}/d\eta)/(N_{\mathrm{part}}/2)$, is shown in the right panel of Fig. 3 for various centrality bins. The uncertainty bands of these distributions also include the Glauber uncertainty on N_{part}. The η dependence of the results is weak, varying by less than

10% over the η range. The slight dip at $\eta = 0$ is a trivial kinematic effect (Jacobian) owing to the use of pseudorapidity (η) rather than rapidity (y). The charged hadron density for the 5% most-central events (0–5% centrality bin) is measured to be $dN_{\mathrm{ch}}/d\eta|_{\eta=0} = 1612 \pm 55$ (syst.) These results are consistent with those of ALICE [19] within the uncertainties.

CMS also measures the p_{T} spectra of charged particles in 2.76 TeV-per-nucleon PbPb collision data [20], with a particular emphasis on the study of the large p_{T} range up to $p_{\mathrm{T}} = 100$ GeV/c. As seen at lower energies [21,22,23,24], the charged particle spectrum in central PbPb collisions turns out to be suppressed by about a factor of 5 compared to binary scaling of nucleon–nucleon collisions around $p_{\mathrm{T}} = 5$–10 GeV/c. Above $p_{\mathrm{T}} = 10$ GeV/c, however, the suppression factor decreases and approaches 2 at $p_{\mathrm{T}} = 40$ GeV/c.

2. Short- and long-range correlation studies

Bose–Einstein Correlations (BEC) have been measured using data collected with the CMS experiment in proton–proton collisions at the LHC, with centre-of-mass energies of 0.9, 2.36 and 7 TeV [25,26]. The BEC signal is observed as an enhancement of pairs of same-sign charged particles with small relative momentum $Q = \sqrt{M^2 - 4m_\pi^2}$, where M is the invariant mass of the two particles, assumed to be pions.

In order to detect the BEC signal, it is convenient to introduce the ratio of the Q distributions for pairs of identical particles in the same event to that for pairs of particles in a reference sample that by construction is expected not to include BEC effects

$$R(Q) = (dN/dQ)/(dN_{\mathrm{ref}}/dQ)\,. \tag{1}$$

The ratio is fitted with the parameterization

$$R(Q) = C\,[1 + \lambda\Omega(Qr)]\;(1 + \delta Q)\,, \tag{2}$$

where $\Omega(Qr)$ is the modulus square of a Fourier transform of the space-time region emitting bosons with overlapping wave functions characterized by an effective size r. The parameter λ measures the strength of BEC for incoherent boson emission from independent sources, δ accounts for long-distance correlations, and C is a normalization factor.

The relevant parameters are quoted using the exponential parameterization for $\Omega(Qr)$. In agreement with previous results, the effective emission radius r is found to increase with $\sqrt{s}$ and to scale with the charged-particle multiplicity in the event. The parameter r turns out to be nearly independent of the average transverse momentum of the pair of particles at the lowest multiplicity range. For the first time in pp interactions, anticorrelations between same-sign charged particles are observed for Q values above

the signal region, as previously reported with LEP data. The anticorrelation effects decrease with increasing charged-particle multiplicity in the event considered in this analysis.

Long-range azimuthal correlations in pp interactions for $2.0 < |\Delta\eta| < 4.8$ have been studied for 7 TeV data, leading to the first observation of a long-range ridge-like structure at the near-side ($\Delta\phi \approx 0$) in pp collisions [27]. This striking feature is clearly seen for large rapidity differences $|\Delta\eta| > 2$ in events with an observed charged particle multiplicity of $N \approx 90$ or higher. The enhancement in the near-side correlation function is most evident in the intermediate transverse momentum range, $1 < p_{\mathrm{T}} < 3$ GeV/c. In the $2.0 < |\Delta\eta| < 4.8$ range, a steep increase of the near-side associated yield with multiplicity has been found in the data, whereas Monte Carlo simulations show an associated yield consistent with zero, independent of multiplicity and transverse momentum.

The hydrodynamic expansion of matter produced in peripheral heavy ion collisions as well as the fluctuation of initial state lead to an azimuthal anisotropy in particle production. CMS studies $\Delta\eta$–$\Delta\phi$ angular correlations between charged particles for different transverse momentum ranges of the trigger ($P_{\mathrm{T}}^{\mathrm{trg}}$) and associated ($P_{\mathrm{T}}^{\mathrm{assoc}}$) particles in a wide centrality range of PbPb collisions at $\sqrt{s} = 2.76$ TeV-per-nucleon [28, 29].

A Fourier decomposition analysis of the 1-D $\Delta\phi$-projected correlation functions in the long-range region ($2 < |\Delta\eta| < 4$) up to the 6-th order harmonics was performed. Evidence of a factorization relation between the Fourier coefficients ($V_{n\Delta}^{\mathrm{f}}$) from dihadron correlations and single-particle azimuthal anisotropy harmonics (v_n^{f}) was observed. The results are summarized in Fig. 4.

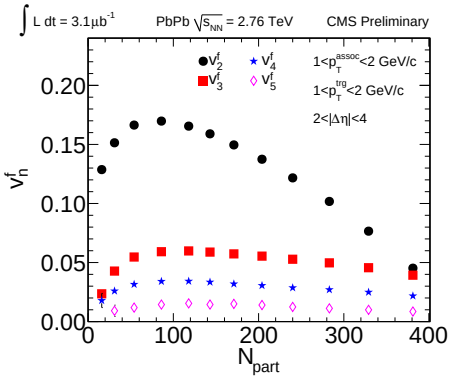

Fig. 4. The flow harmonics v_2^{f}, v_3^{f}, v_4^{f} and v_5^{f} extracted from long-range ($2<|\Delta\eta|<4$) azimuthal dihadron correlations for $1<p_{\mathrm{T}}^{\mathrm{trg}} < 2$ GeV/c and $1 < p_{\mathrm{T}}^{\mathrm{assoc}} < 2$ GeV/c as a function of the number of participating nucleons N_{part} in PbPb collisions at $\sqrt{s} = 2.76$ TeV-per-nucleon.

3. Underlying Event measurements

This section summarizes the CMS Underlying Event (UE) studies in pp interactions up to highest centre of mass energies of 7 TeV. The Underlying Event in Drell–Yan and jet events is studied measuring the charged multiplicity density and the charged energy density in different regions which are defined considering the azimuthal distance of the reconstructed tracks with respect to the reconstructed boson and leading track-jet, respectively. Complementary measurements in the transverse region and a methodology using the jet median/area approach are also discussed. We compare our underlying event results with the predictions from different Monte Carlo event generators and tunes.

In the presence of a hard process, characterized by the presence of particles or clusters of particles with a large transverse momentum p_{T} with respect to the beam direction, the final state of hadron–hadron interactions can be described as the superposition of several contributions: products of the partonic hard scattering with the highest scale, including initial and final state radiation; hadrons produced in additional MPI; and "beam–beam remnants" (BBR) resulting from the hadronization of the partonic constituents that did not participate in other scatterings. Products of MPI and BBR form the UE. The UE cannot be uniquely separated from initial and final state radiation.

The traditional CMS UE measurement in jet final states [30] concentrates on the study of the transverse region, which is defined considering the azimuthal distance of the reconstructed tracks with respect to the leading track-jet of the event: $60^\circ < |\Delta\phi| < 120^\circ$. The jet reconstruction algorithm used in these studies is SisCone [31].

Generator level Monte Carlo predictions according to different programs and tunes are compared to the data corrected with a Bayesian unfolding technique taking into account the detector effects [6]. The PYTHIA 6 [32, 33] tune Z1 [30] adopts p_{T} ordering of parton showers and the new PYTHIA MPI model [34]. It includes the results of the Professor tunes [35] considering LEP fragmentation and the color reconnection parameters of the AMBT1 tune [36], while with the early CMS UE results have been used to tune the parameters governing the value and the $\sqrt{s}$ dependence of the cut-off transverse momentum that in PYTHIA regularizes the divergence of the leading order scattering amplitude as the final state parton transverse momentum $\hat{p}_{\mathrm{T}}$ approaches 0. PYTHIA 8 [37,38] also uses the new PYTHIA MPI model, which is interleaved with parton showering. The PYTHIA 8 tune 4C [39] which focuses on the description of the early LHC data, is adopted here.

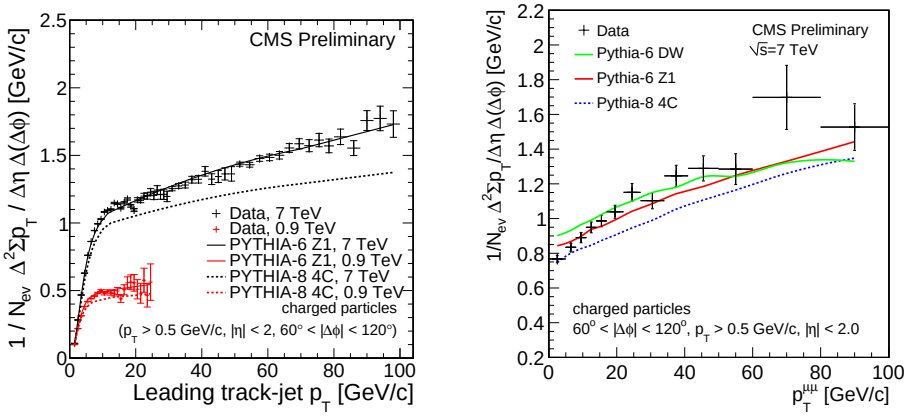

Fig. 5. Average scalar $\sum p_{\mathrm{T}}$ for tracks with a pseudorapidity $|\eta| < 2.0$ and $p_{\mathrm{T}} > 0.5$ GeV/c in the transverse region as a function of the (left) leading track-jet p_{T}, for data at $\sqrt{s} = 0.9$ TeV and $\sqrt{s} = 7$ TeV; (right) $p_{\mathrm{T}}^{\mu\mu}$, for data at $\sqrt{s} = 7$ TeV. Predictions from different PYTHIA 6 and PYTHIA 8 tunes are compared to the corrected data. The inner error bars indicate the statistical uncertainties affecting the measurements, the outer error bars thus represent the statistical uncertainties on the measurements and the systematic uncertainty affecting the Monte Carlo predictions added in quadrature.

The centre-of-mass energy dependence of the hadronic activity in the transverse region is presented in Fig. 5 (left) as a function of the p_{T} of the leading track-jet. The data points represent the average scalar track-p_{T} sum dependence, for $\sqrt{s} = 0.9$ TeV and $\sqrt{s} = 7$ TeV using tracks with a pseudorapidity $|\eta| < 2.0$ and $p_{\mathrm{T}} > 0.5$ GeV/c. A significant growth of the UE activity of charged particles transverse to that of the leading track-jet is observed with increasing scale provided by the leading track-jet p_{T}, followed by saturation at large values of the scale. A significant growth of the activity in the transverse region is also observed, for the same value of the leading track-jet p_{T}, from $\sqrt{s} = 0.9$ TeV to $\sqrt{s} = 7$ TeV. These observations are consistent with the ones obtained at Tevatron [40]. The evolution with the hard scale of the ratio of the UE activity at 7 TeV and 0.9 TeV is remarkably well described by the Z1 tune. The trend is also reproduced by PYTHIA 8 Tune 4C. The strong growth of UE activity with charged particles is also striking in the comparison of the distributions of charged particle multiplicity, p_{T} and scalar p_{T} sum (not shown here) which corroborate the presence of a hard component in the UE hence the adoption of the MPI models.

The Drell–Yan (DY) process with muonic final state, $q\bar{q} \to \mu^+\mu^-$, provides an excellent complementary way to study the underlying event. The CMS UE measurement [41] in DY events focuses on the di-muon invariant mass region between 60 and 120 GeV/c^2. The UE observables defined in the jet final states are extended to the DY case replacing the track-jet with the di-muon. Figure 5 (right) shows the scalartrack-p_{T} sum using tracks with a pseudorapidity $|\eta| < 2.0$ and $p_{\mathrm{T}} > 0.5$ GeV/c in the transverse region. Since the minimum energy scale of the event in this analysis is set by the lower bound on $M_{\mu\mu}$, the MPI component turns out to be saturated, hence only a small but noticeable growth of the UE activity with increasing $p_{\mathrm{T}}^{\mu\mu}$ can be observed which can be attributed to the radiative component. The UE measurement in DY events is extended to the regions along and opposite with respect to the di-muon direction (not shown here). Extrapolating to the point with minimal radiative and maximal MPI contribution, the UE activity in DY events turns out to be around 25% lower with respect to the jet case. In Ref. [42] this is interpreted in terms of the reduced transverse size of the gluons with respect to the quarks.

On top of the traditional approach, a new methodology to quote the UE adopting anti-k_{T} jets [43] and relying on the measurement of their area [44] is adopted for the first time by CMS using charged particles in pp collision data collected at $\sqrt{s} = 0.9$ TeV [45]. The new set of UE observables consider the whole pseudorapidity-azimuth plane instead of the transverse region and inherently take into account the leading jets of an event.

CMS also reports measurements of the energy flow in the forward region [46, 47] for minimum bias, dijet and DY events. These measurements are connected to the central region UE ones as the basic philosophy is the same: they concentrate on the complementary activity of a pp interaction for different energy scales of the reconstructed leading objects.

REFERENCES

[1] R. Adolphi *et al.*, *JINST* **3**, S08004 (2008).

[2] V. Khachatryan *et al.*, *J. High Energy Phys.* **02**, 041 (2010) [arXiv:1002.0621v2 [hep-ex]].

[3] V. Khachatryan *et al. Phys. Rev. Lett.* **105**, 022002 (2010) [arXiv:1005.3299v2 [hep-ex]].

[4] S. Chatrchyan *et al.*, *J. High Energy Phys.* **08**, 086 (2011) [arXiv:1104.3547v2 [hep-ex]].

[5] V. Khachatryan *et al.*, *J. High Energy Phys.* **1101**, 079 (2011) [arXiv:1011.5531v1 [hep-ex]].

[6] G. D'Agostini, *Nucl. Instrum. Methods* **A362**, 487 (1995).

[7] J.F. Grosse-Oetringhaus, K. Reygers, *J. Phys. G* **37**, 083001 (2010) [arXiv:0912.0023v2 [hep-ex]].

[8] Z. Koba, H.B. Nielsen, P. Olesen, *Nucl. Phys.* **B40**, 317 (1972).

[9] S. Hegyi, *Nucl. Phys. Proc. Suppl.* **92**, 122 (2001) [arXiv:hep-ph/0011301v1].

[10] V. Khachatryan *et al.*, *J. High Energy Phys.* **05**, 064 (2011) [arXiv:1102.4282v2 [hep-ex]].

[11] K. Aamodt *et al.*, *Eur. Phys. J.* **C71**, 1594 (2011) [arXiv:1012.3257v2 [hep-ex]].

[12] B.I. Abelev *et al.*, *Phys. Rev.* **C75**, 064901 (2007) [arXiv:nucl-ex/0607033v1].

[13] D. Acosta *et al.*, *Phys. Rev.* **D72**, 052001 (2005) [arXiv:hep-ex/0504048v1].

[14] T. Aaltonen *et al.*, arXiv:1101.2996v1 [hep-ex].

[15] S. Chatrchyan *et al.*, *J. High Energy Phys.* **08**, 141 (2011) [arXiv:1107.4800v2 [nucl-ex]].

[16] M.L. Miller *et al.*, *Annu. Rev. Nucl. Part. Sci.* **57**, 205 (2007).

[17] B. Alver *et al.*, arXiv:0805.4411v1 [nucl-ex].

[18] S. Chatrchyan *et al.*, *Phys. Rev.* **C84**, 024906 (2011) [arXiv:1102.1957v2 [nucl-ex]].

[19] ALICE Collaboration, *Phys. Rev. Lett.* **106**, 032301 (2011).

[20] Nuclear Modification Factor for Charged Hadron Production at High p_{T} in PbPb Collisions at $\sqrt{s_{NN}} = 2.76$ TeV, CMS Physics Analysis Summary, CMS-PAS-HIN-10-005, 2010.

[21] J. Adams *et al.*, *Nucl. Phys.* **A757**, 102 (2005) [arXiv:nucl-ex/0501009v3].

[22] K. Adcox *et al.*, *Nucl. Phys.* **A757**, 184 (2005) [arXiv:nucl-ex/0410003v3].

[23] I. Arsene *et al.*, *Nucl. Phys.* **A757**, 1 (2005) [arXiv:nucl-ex/0410020v1].

[24] B.B. Back *et al.* [PHOBOS Collaboration], *Nucl. Phys.* **A757**, 28 (2005) [arXiv:nucl-ex/0410022v2].

[25] V. Khachatryan *et al.*, *Phys. Rev. Lett.* **105**, 032001 (2010) [arXiv:1005.3294v1 [hep-ex]].

[26] V. Khachatryan *et al.*, *J. High Energy Phys.* **1105**, 029 (2011) [arXiv:1101.3518v1 [hep-ex]].

[27] V. Khachatryan *et al.*, *J. High Energy Phys.* **1009**, 091 (2010) [arXiv:1009.4122v1 [hep-ex]].

[28] S. Chatrchyan *et al.*, [arXiv:1105.2438v1 [nucl-ex]].

[29] Centrality and Multiplicity Dependence of Dihadron Correlations in PbPb and *pp* Collisions, CMS Physics Analysis Summary, CMS-PAS-HIN-11-006, 2010.

[30] S. Chatrchyan *et al.*, *J. High Energy Phys.* **09**, 109 (2011) [arXiv:1107.0330v1 [hep-ex]].

[31] G.P. Salam, G. Soyez, *J. High Energy Phys.* **0705**, 086 (2007) [arXiv:0704.0292v2 [hep-ph]].

[32] T. Sjostrand, M. van Zijl, *Phys. Lett.* **B188**, 149 (1987).

[33] T. Sjostrand, S. Mrenna, P.Z. Skands, *J. High Energy Phys.* **0605**, 026 (2006) [arXiv:hep-ph/0603175v2].

[34] P.Z. Skands, D. Wicke, *Eur. Phys. J.* **C52**, 133 (2007) [arXiv:hep-ph/0703081v2].

[35] A. Buckley *et al.*, *Eur. Phys. J.* **C65**, 331 (2010) [arXiv:0907.2973v1 [hep-ph]].

[36] G. Aad *et al.*, *New J. Phys.* **13**, 053033 (2011) [arXiv:1012.5104v2 [hep-ex]].

[37] T. Sjostrand, arXiv:0809.0303v1 [hep-ph].

[38] R. Corke, arXiv:0901.2852v1 [hep-ph].

[39] R. Corke, T. Sjostrand, *J. High Energy Phys.* **1103**, 032 (2011) [arXiv:1011.1759v1 [hep-ph]].

[40] T. Affolder *et al.*, *Phys. Rev.* **D65**, 092002 (2002).

[41] Measurement of the Underlying Event Activity in the Drell–Yan process in Proton–Proton Collisions at $\sqrt{s} = 7$ TeV, CMS Physics Analysis Summary, CMS-PAS-QCD-10-040, 2010.

[42] L. Frankfurt, M. Strikman, C. Weiss, *Phys. Rev.* **D83**, 054012 (2011) [arXiv:1009.2559v1 [hep-ph]].

[43] M. Cacciari, G.P. Salam, G. Soyez, *J. High Energy Phys.* **0804**, 063 (2008) [arXiv:0802.1189v2 [hep-ph]].

[44] M. Cacciari, G.P. Salam, S. Sapeta, *J. High Energy Phys.* **1004**, 065 (2010) [arXiv:0912.4926v2 [hep-ph]].

[45] Measurement of the Underlying Event Activity with the Jet Area/Median Approach at 0.9 TeV, CMS Physics Analysis Summary, CMS-PAS-QCD-10-005, 2010.

[46] S. Chatrchyan *et al.*, arXiv:1110.0211v1 [hep-ex].

[47] S. Chatrchyan *et al.*, arXiv:1110.0181v1 [hep-ex].